Development of a Two-Joint Robotic Fish for Real-World Exploration

Jianhong Liang, Tianmiao Wang, and Li Wen
Robotics Institute, Beihang University, 37 Xueyuan Road, Beijing 100191, People's Republic of China
e-mail: dommy_leung@263.net

Received 16 February 2010; accepted 18 July 2010

Research on biomimetic robotic fish has been undertaken for more than a decade. Various robotic fish prototypes have been developed around the world. Although considerable research efforts have been devoted to understanding the underlying mechanism of fish swimming and construction of fish-like swimming machines, robotic fish have largely remained laboratory curiosities. This paper presents a robotic fish that is designed for application in real-world scenarios. The robotic fish adopts a rigid torpedo-shaped body for the housing of power, electronics, and payload. A compact parallel four-bar mechanism is designed for propulsion and maneuvering. Based on the kinematic analysis of the tail mechanism, the motion control algorithm of joints is presented. The swimming performance of the robotic fish is investigated experimentally. The swimming speed of the robotic fish can reach 1.36 m/s. The turning radius is 1.75 m. Powered by the onboard battery, the robotic fish can operate for up to 20 h. Moreover, the advantages of the biomimetic propulsion approach are shown by comparing the power efficiency and turning performance of the robotic fish with that of a screw-propelled underwater vehicle. The application of the robotic fish in a real-world probe experiment is also presented.

1. INTRODUCTION

The study of swimming mechanisms of fish and the development of bionic engineering have shown that biorobotic underwater vehicles have potential advantages in terms of maneuverability, environmental suitability, and low noise. The fin-powered Transphibian robot developed by iRobot can be used as an autonomous unmanned undersea vehicle (UUV) and bottom crawler, and it shows potential application in mine detection, harbor defense, surveillance, and reconnaissance (iRobot Maritime Robots—Transphibian, 2010). Hu, Liu, Duks, and Francis (2006) are trying to develop a carp-like robotic fish to find the source of potentially hazardous pollutants in the water. Mbemmo, Chen, Shatara, and Tan (2008) built a robotic fish propelled with an ionic polymer metal composite (IPMC) actuator. The above research suggests that bionic underwater vehicles are increasingly being used in a variety of practical applications. However, several technical questions need to be dealt with if the robotic fish is to be employed in real-world applications, such as whether the swing machinery can withstand hydraulic pressure when submerged in deep water and whether the reciprocating mechanism that drives the flapping fin is power efficient when compared to the mechanism that drives a screw propeller.

The SPC series robotic fish developed at the Robotics Institute of Beihang University is a biorobotic autonomous underwater vehicle targeted for real-world exploration. The main features of SPC robotic fish include operation in deep water by adopting a rigid hull and mechanical seal widely used on traditional UUVs, as well as high efficiency through utilization of dc servomotor actuation whose efficiency of electromechanical energy conversion is very high. Only two joints are employed at the caudal fin thruster in order to reduce the thruster's fraction of the hull volume. The SPC-I robotic fish is used to study the impact of yaw stability on tail fin propulsion (Wang & Liang, 2005). SPC-II is used to study hovering and turning maneuverability. It achieves a turning rate of 30 deg/s, and the minimum turning radius is about half its body length. In 2004 the SPC-II robotic fish was deployed in an underwater archaeology mission undertaken by the Underwater Archaeological Team of the National Museum of China at Dongshan Island in Fujian Province (Liang, Wang, Wang, Zou, & Sun, 2005). SPC-III adopts the same torpedo body shape as a conventional UUV and has a two-joint caudal fin thruster that can be easily replaced with a screw propeller. With the same hydrodynamic shape of the hull, experimental results of the performance of fin and propeller propulsion are compared. Through improvement of the mechanical structure and motion control algorithm, the SPC-III robotic fish achieves higher propulsion efficiency than any previous SPC robotic fish.

The remainder of the paper is organized as follows. Section 2 introduces the design and improvement of SPC-III robotic fish. The motion control algorithm of the caudal fin is addressed in Section 3. Section 4 presents test results

Multimedia files may be found in the online version of this article.

of velocity and efficiency of the robotic fish, both of which are compared with that of a screw-propelled UUV. Section 5 gives the result of a long-distance probe experiment in a real-world scenario with the robotic fish. Section 6 is a discussion. Finally, we conclude the paper with an outline of future work in Section 7.

2. DEVELOPMENT OF SPC-III ROBOTIC FISH AND COMPARISON UUV

2.1. Design and Improvement of SPC-III Robotic Fish

The SPC-III robotic fish is a biorobotic UUV designed for exploration missions that require a robot to withstand pressure exerted in a depth of up to 50 m. As shown in Figure 1(b), the front and middle sections of the robot are a rigid hull fabricated with carbon fiber and aluminum alloy materials. The rear section is a caudal fin thruster, and the hull of the thruster is molded with engineering plastics due to its complex shape. The SPC series robotic fish have two important features. First, the caudal fin thruster is not covered by any flexible exostructure. The caudal fin's drive link assembly, which is compact and lightweight, is directly exposed to water. As a result, conventional pressure hull and sealing methods can be adopted. This means that the power consumed by the deformation of the flexible exostructure can be avoided. Second, the caudal fin is driven by two dc servomotors with which precise motion control of the caudal fin can be realized. Moreover, it is convenient to compare the efficiency of the caudal fin thruster with that of a screw propeller that also is driven by dc servomotors.

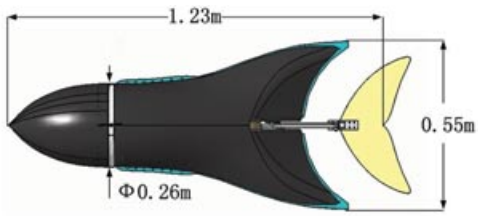

(a) SPC-II adopts two RE40 servomotors to drive the caudal fin thruster; the reduction ratio is 43

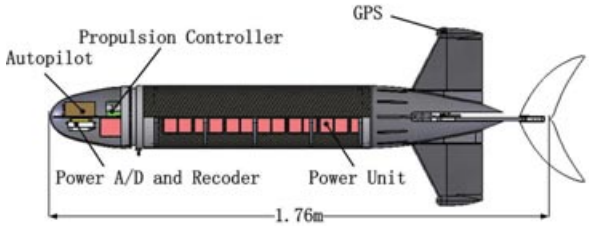

(b) SPC-III adopts two RE40 servomotors to drive the caudal fin thruster; the reduction ratio is 30

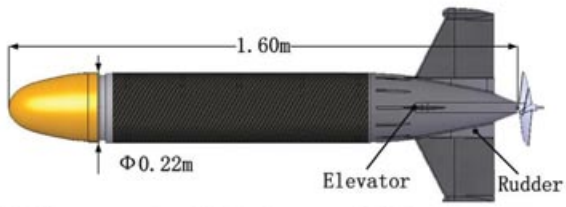

(c) The comparison UUV adopts one RE40 servomotor to drive screw propeller; the reduction ratio is 5.

Figure 1. SPC-II and SPC-III robotic fish and the comparison UUV.

Compared with SPC-II robotic fish [see Figure 1(a)], SPC-III is an improvement in several ways. The first improvement is the shape of the hull. By adopting a torpedo shape, the diameter of the cylindrical hull is decreased to 0.22 m and the cross-sectional area of SPC-III is decreased about 29% with the same displacement. Different from traditional UUVs, SPC-III has large dorsal and ventral fins at the caudal section to balance the side force produced by the flapping caudal fin. As a result, the yaw angle is restricted within 3 deg when the tail flaps. SPC-II uses two Maxon RE40 servomotors to drive the tail fin. The planetary gear box with a reduction ratio of 43 adopted in SPC-II can reach its nominal transmission efficiency of 83% only when the output power is maximal; the transmission efficiency falls below 70% when the output power is low. Because a screw propeller adopts a direct-drive method or planetary gear box of low reduction ratio that can realize high transmission efficiency, the drive mechanism of the caudal fin must be improved to achieve lower power loss. Thus, a spur gear box with reduction ratio of 30 is custom-made. In addition, a titanium alloy shaft with diameter of 0.1 m is employed for high mechanical strength. Figure 2 shows zero-load powers of SPC-II and SPC-III robotic fish, which are measured with the power measurement system described in Section 4.1. The zero-load power is measured with the caudal fin uninstalled and corresponds to the power consumed by the the motor, amplifier, and mechanical drive

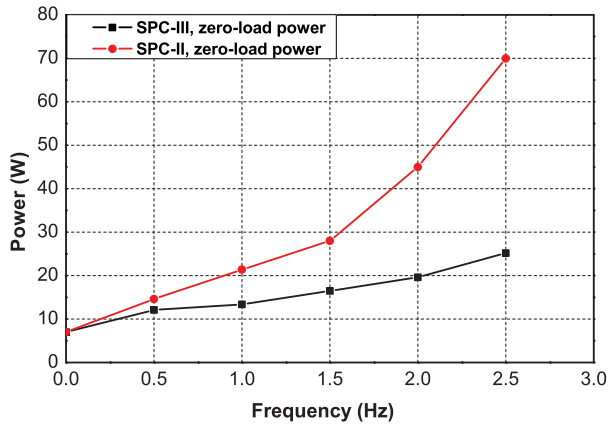

Figure 2. Zero-load powers of SPC-II and SPC-III robotic fish.

Table I. Parameter comparisons between the screw propeller and the caudal fin thruster.

Caudal fin thruster		Screw propeller	
Parameter	Value	Parameter	Value
Area of caudal fin S (mm^2)	25,287	Diameter D (mm)	240
Maximum chord length c_0 (mm)	120	Number of blades Z	3
Average chord length c (mm)	70	Expanded area ratio A_E/A_0	0.36
Lead edge sweepback (deg)	47	Pitch ratio $(P/D)_{0.7R}$	0.837
Airfoil	1-mm flat plate	Airfoil	NACA66mod $a = 0.8$
Length of link 1, 3 (mm)	280	Hub radial ratio d_h/D	0.18
Length of link 2, 4 (mm)	28	Rotation direction	Right
Driving motors	RE40 (150 W) × 2	Driving motors	RE40 (150 W) × 1
Reduction ratio	$i = 30$ (2 grade spur gear)	Reduction ratio	$i = 5$ (1 grade planetary gear)
Weight (kg)	3.3	Weight (kg)	2.1

Figure 3. Mechanical configuration of the screw propeller.

linkage. This shows that the power loss induced by the drive mechanism is decreased significantly.

As shown in Figure 1(b), the front section of SPC-III houses equipment and payload. An autopilot IFLY40, which is used to control small unmanned aerial vehicles (UAVs), is installed at the front hull for navigation and control of SPC-III. IFLY40 was successfully applied in the 24th Chinese National Antarctic Research Expedition in December 2007 (Chen, Wang, Liang, & Wang, 2008), finishing the task of sea ice investigation. It can provide the data of posture, course angle, global positioning system (GPS), and altitude and has five proportional–integral–derivative (PID) controllers. The barometric sensor for UAVs is replaced with a water pressure sensor, which provides in-depth data from up to 50 m below the water level. Below the autopilot is an A/D converter and data recorder, and the motion controller of the caudal fin thruster is located in the back. The middle section of the hull is for the power unit, which is composed of 14 168-Wh Li-poly batteries and provides energy for long endurance. On the top of the dorsal fin is a GPS antenna for the autopilot.

2.2. Development of Propeller-Driven Comparison UUV

There has been a long-standing question in the field of fish robotics as to how an oscillating tail fin stacks up against a conventional screw propeller. In this research, the performances of both underwater propulsion methods are tested and compared. A comparison UUV was built by directly replacing the caudal fin thruster of SPC-III with a screw propeller [see Figure 1(c)] while the other components remained unchanged. The propeller was designed and fabricated with the help of the China Ship Scientific Research Center (CSSRC). The open water efficiency η_0 of the propeller at a speed of 5 kn is predicted to be 0.67 (Ying & Zhu, 2006). Figure 3 shows the mechanical configuration of the screw propeller. Parameter comparisons between the screw propeller and the caudal fin thruster are shown in Table I.

3. MOTION CONTROL OF CAUDAL FIN THRUSTER

3.1. Caudal Fin Thruster and Its Control Law

As shown in Figure 4, the caudal fin that generates thrust forces is attached at the end of the drive link assembly. The caudal fin is made of 1-mm-thick carbon fiber and imitates the shape of a tuna's caudal fin, but with a lower aspect ratio. The dimensions of the caudal fin are shown in Table I. Both link 1 and link 2 are driven by Maxon RE40 servomotors that pass through reducers with a reduction ratio of 30. The two servomotors are installed coaxially, constituting a two-degree-of-freedom parallel manipulator. Through the four-bar parallel mechanism, the two servomotors can precisely control the motion of the caudal fin. This design allows the drive mechanism of the caudal fin to be both simple and lightweight. The weight of the drive link assembly and caudal fin combined is 648 g, occupying 1.4% of the total displacement. This design can also reduce the power loss induced by mechanical vibration.

As shown in Figure 4(c), let A be the flapping amplitude of the caudal fin, α the attack angle, L the length of link 1, and θ_1 and θ_2 the rotating angles of link 1 and link 2, respectively. Then the following relationship can be obtained:

$$\begin{aligned} A &= L \sin\theta_1, \\ \alpha &= \theta_2. \end{aligned} \tag{1}$$

In steady swimming, the performance of the caudal fin is affected by the following parameters:

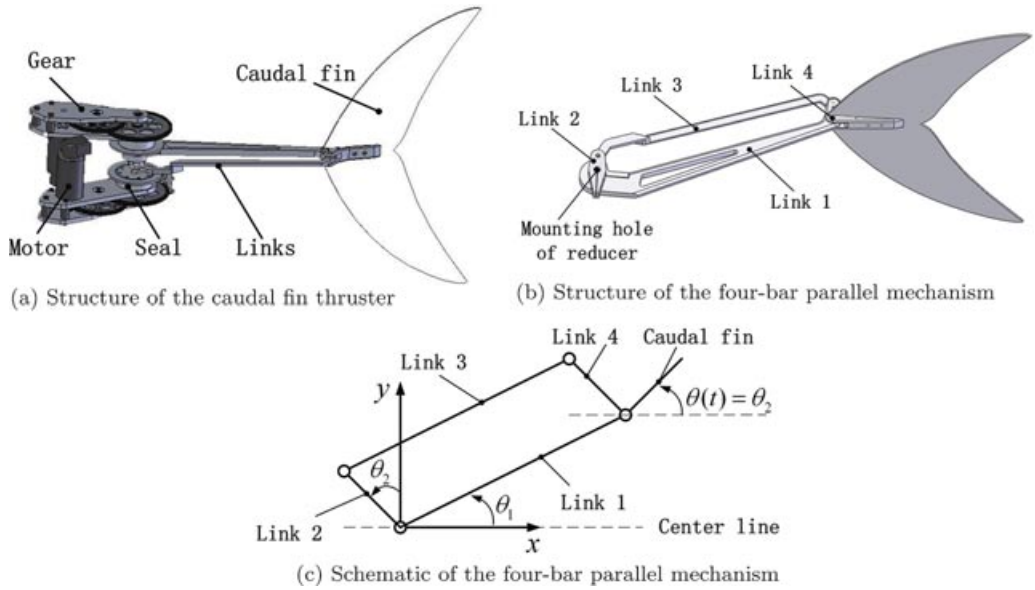

(a) Structure of the caudal fin thruster

(b) Structure of the four-bar parallel mechanism

(c) Schematic of the four-bar parallel mechanism

Figure 4. Mechanical configuration of the caudal fin thruster.

1. Dimensionless flapping amplitude, defined as $H = A_0/c_0$, where A_0 is the peak-to-peak amplitude and c_0 is the maximum chord length.
2. The maximum angle of attack, denoted as α_0.
3. The phase difference φ between the heave and pitch motion.
4. The Strouhal number, defined as $St = fA_0/V$, where V is the speed of inflow.

The motion control law of the caudal fin can thus be expressed as

$$\begin{aligned} A &= \tfrac{1}{2}A_0\cos(2\pi t), \\ \alpha &= \alpha_0\cos(2\pi t - \varphi). \end{aligned} \tag{2}$$

It is clear that accurate adjustment of the former three parameters can be realized by adjusting the motion law of θ_1 and θ_2. In the control system of the caudal fin thruster, a two-axis motion coordinator is used to generate the above motion law. Anderson, Streitlien, Barrett, and Triantafyllou (1998) and Barrett and Triantafyllou (1999) presented the optimum ranges of the four parameters. However, in the realization of the control algorithm of the caudal fin, the actual motion is distorted due to the resistance force, which reduces the propulsive efficiency.

3.2. Lookup-Table Method and Predictive Control

3.2.1. Motion Control Based on Lookup-Table Method

The position and velocity of the motors at each discrete time instant of an oscillating period are stored in the controller of the SPC-II in advance. With the real-time angle information of link 1, the stored data are retrieved and used to coordinate the motion of the two joints.

It can be derived from Figure 4 that

$$\theta_1 = A_1\cos 2\pi f t, \tag{3}$$

$$\theta_2 = A_2\cos(2\pi f t - \varphi), \tag{4}$$

where A_1 is the flapping amplitude of link 1, A_2 is the flapping amplitude of link 2, and f is the flapping frequency of the caudal fin. Taking derivatives and using triangulation on the above two equations, the rotating speed of link 1 and the angle of link 2 can be expressed as follows:

$$n_1 = 2\pi f\sqrt{A_1^2 - \theta_1^2}, \tag{5}$$

$$\theta_2 = \frac{A_2}{A_1}\left(\theta_1\cos\varphi - \frac{n_1}{2\pi f}\sin\varphi\right), \tag{6}$$

where n_1 is the set rotational speed of the motor that drives link 1. A table that correlates θ_1, n_1, and θ_2 can be established from Eqs. (5) and (6). Motion control of the caudal fin can be achieved by looking up the table. The advantages of the lookup-table method are its simple implementation and fewer computation requirements to the motion controller. However, with the increase of flapping frequency, more data are skipped between two control periods by the motion controller, making the motion profile distorted. Also, the mechanical system cannot reach the desired speed or position immediately after the control parameters are assigned, which introduces an uncertain lag and more distortion.

3.2.2. Predictive Control Based on Real-Time Computing

The motion control algorithm of SPC-III robotic fish has been improved to deal with distortions. The current angle

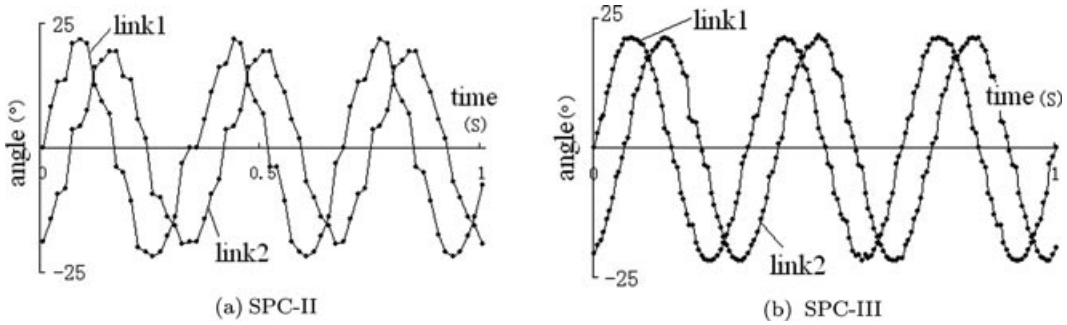

Figure 5. Flapping profiles of SPC-II and SPC-III robotic fish.

of link 1 is used to calculate the desired speed. Then compensation is introduced, which makes the actual speed of the motor reach the desired speed after a computation cycle. The set rotational speed n_{1_st} of link 1 is described in Eq. (7):

$$n_{1\_st} = n_{1th} + \Delta n_1, \tag{7}$$

where n_{1th} is the desired speed obtained from Eq. (5) and Δn_1 is a small constant compensation based on the flapping tendency.

To deal with the distortion of link 2, a predictive control method is employed. Given the set rotational speed n_{1_st} of link 1, the angle of link 1 after a computation cycle time T can be obtained from

$$\theta_{1\_f} = \theta_{1ac} + n_{1th}T, \tag{8}$$

where θ_{1_f} is the angle of link 1 after a computation cycle and θ_{1ac} is the current position of link 1. Then the position of link 2 can be calculated as

$$\theta_{2\_d} = \frac{A_2}{A_1}\left(\theta_{1\_f}\cos\varphi - \frac{n_{1\_st}}{2\pi f}\right)\sin\varphi. \tag{9}$$

Figure 5 shows the flapping profiles of SPC-II and SPC-III with these two control methods. It is clear that SPC-III can follow the set motion profile more precisely.

4. PROPULSION EXPERIMENT AND COMPARISON STUDY

4.1. Measurement Systems

Control and data measurement of SPC-III robotic fish are achieved with the IFLY40 autopilot using its telemetry function. Figure 6 shows the electrical system of SPC-III robotic fish. In this study, the power of the propeller and speed and maneuverability of the vehicle are measured and sent to the ground station. The transmission speed is adjustable within the range of 1–10 frames per second.

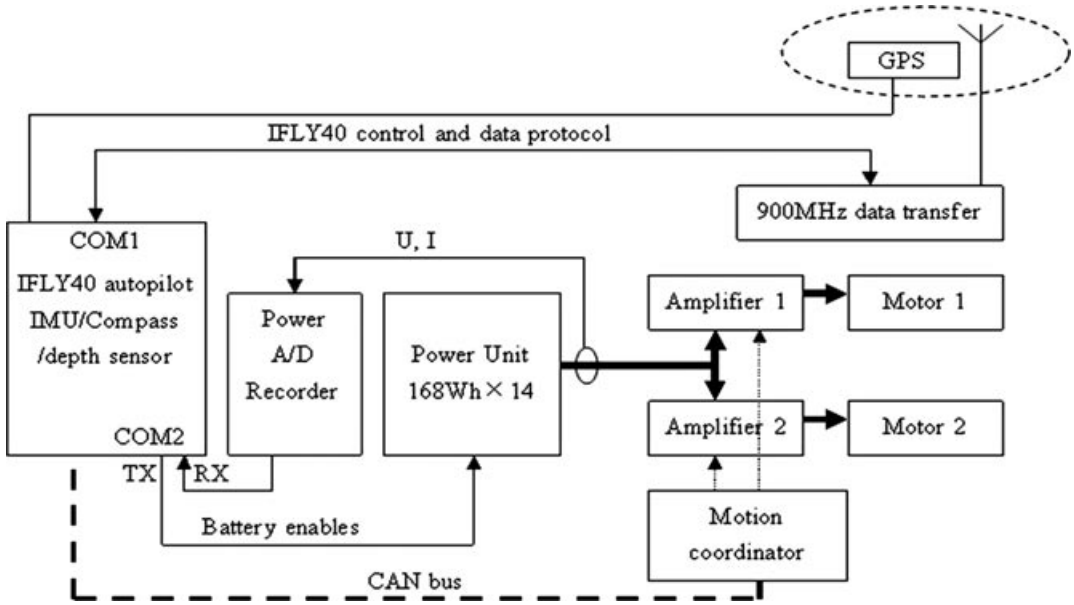

Figure 6. Electrical system of SPC-III robotic fish.

Vehicle velocity measurement: The IFLY40 autopilot can operate in several modes such as UAV mode and remotely piloted vehicle (RPV) mode, which enables the vehicle to maintain direction on the route of an experiment for a long time. In this experiment, the voyage and speed of the vehicle are calculated with the longitude and latitude data provided by the autopilot. The positioning error of the onboard GPS is within 2.5 m. Comparatively accurate average speed can be achieved when the traveled distance is long enough. The distance and speed of the vehicle are computed using data of 200 s.

Power measurement: An embedded computer with a 16-bit, eight-channel A/D converter is adopted for the measurement of power. The sampling frequency is 100 Hz, and the integration of power is carried out every second. The data are sent by the autopilot every second and recorded by the ground station. Similar to the measurement of velocity, the average power is calculated with data of 200 s. The current and voltage are measured on the circuit between the batteries and the amplifier. Therefore the measured power is the total power consumed by the propulsion system.

Yaw rate measurement: In the measurement of maneuverability, the sampling frequency is increased to 10 Hz. The IFLY40 autopilot can output the heading angle of the vehicle, which is measured by GPS and the electronic compass.

4.2. Comparison of Propulsion Performance

Experiments with SPC-III robotic fish and the comparison UUV were carried out on the beach of Qinhuangdao located on the west coast of Bohai Sea. Figure 7 shows the comparison UUV and SPC-III biorobotic UUV settled in cradles on the beach. The static power and zero-load power are measured first. Results show that the power consumed by the caudal fin thruster and the screw propeller at static state is 7 and 3.5 W, respectively, corresponding to the

Figure 7. The comparison UUV (with propeller, left) and SPC-III biorobotic UUV (with fin, right) settled in cradles on the beach.

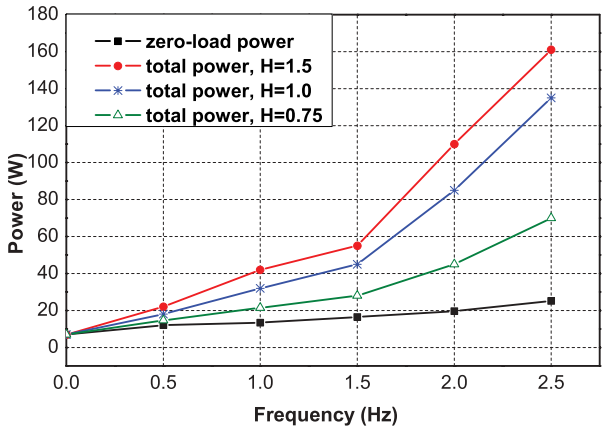

Figure 8. Zero-load and total power of caudal fin.

power of two amplifiers and one amplifier. Because of more complicated mechanical structures, the zero-load power of the caudal fin thruster is higher than that of the screw propeller. The former is 25 W with flapping frequency of 2.5 Hz (see Figure 8), and the latter is 18 W at a rotational speed of 10 rps (rounds per second) (see Figure 9).

To measure speed and power in water, the posture of the vehicle is adjusted to be level. To ensure that the GPS can receive stable signals and the data radio can work in good condition, the weight of the vehicle is adjusted so that the GPS antenna located on top of the dorsal fin is 0.2 m above the water. To avoid influence of the control system, manually adjusting the neutral position of the caudal fin or the bias angle of the rudder rather than using the course control function of the autopilot realizes the linear trajectory of the vehicle.

The power and velocity of the vehicle are tested continuously. After the autopilot is set with new control parameters through the ground station, the trajectory of the vehicle is adjusted carefully to ensure linear swimming. The stable state lasts for a few minutes to allow the GPS time to be recorded. The test data can be retrieved according to

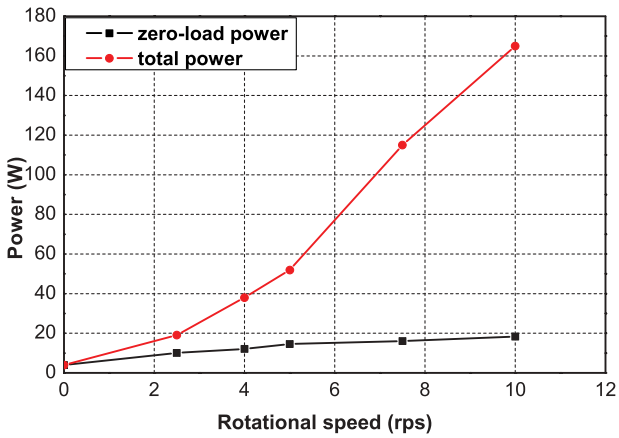

Figure 9. Zero-load and total power of screw propeller.

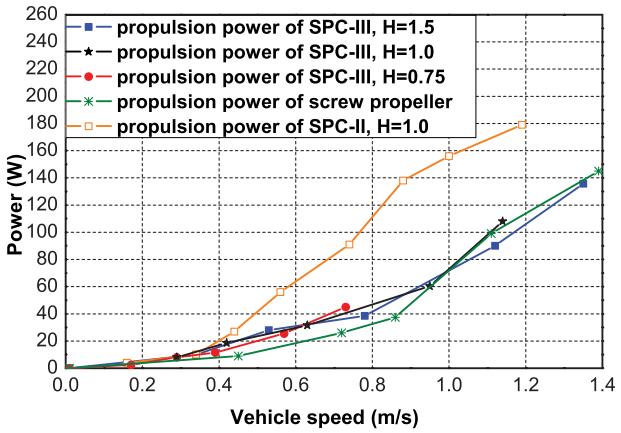

Figure 10. Propulsion power of SPC-III, SPC-II, and screw propeller at different swimming speeds.

the GPS time for postprocessing. To compare the power consumptions of the caudal fin and the screw propeller, we define propulsion power as the total power of the propulsion system minus the zero-load power. As shown in Figures 8–10, the final test results indicate that with a flapping frequency of 2.5 Hz and $H = 1.5$, the caudal fin thruster achieves a maximum speed of 1.36 m/s with a propulsion power of 136 W. The screw propeller achieves a maximum speed of 1.4 m/s at the rotational speed of 10 rps and with propulsion power of 145 W. At a lower swimming speed, the caudal fin thruster achieves 1.10 m/s with a flapping frequency of 2 Hz and propulsion power of 90 W, whereas the screw propeller achieves 1.12 m/s with a rotational speed of 7.5 rps and propulsion power of 99 W. The pitch of the vehicle becomes unstable when the flapping frequency or rotational speed is increased for a higher speed, also preventing the GPS from working normally.

A fundamental principle of adjusting flapping parameters of the caudal fin is to generate larger thrust forces for comparison with the screw propeller. Owing to deformation of the carbon fiber caudal fin, the motion control parameters are inconsistent with the parameters of the rigid fin used in earlier work. The deformation can lead to an increase in attack angle and phase lag. Maximum swimming speed is achieved with $\alpha = 10$ deg and $\phi = 45$ deg. Experiments are carried out with $H = 0.75$, 1.0, and 1.5, respectively. With the same flapping frequency, the output power is higher with $H = 1.5$, associated with lower total power consumption at the same swimming speed. With $H = 0.75$, the thrust force is relatively small and the maximum speed is only 0.75 m/s.

As shown in Figure 10, the propulsion power of SPC-III is much less than that of SPC-II, which can be attributed to smaller resistance and tail fin area. The caudal fin thruster consumed less power when $f > 1$ Hz and $H = 1.5$ than the screw propeller. Particularly when $f = 2$ Hz, $H = 1.5$, and $v = 1.1$ m/s, the caudal fin thruster consumed about 7% less power than the screw propeller.

4.3. Maneuverability Performance

Potential applications of portable AUVs include reconnaissance of port and coast. To perform these tasks, AUVs often need to be close to the object and at the same time avoid colliding. In such circumstances, low-speed maneuverability is particularly important. For example, an AUV is often constrained in narrow space when it operates autonomously. The AUV needs to turn around in order to go back to the open sea. Such maneuvering is often used by remotely operated vehicles (ROVs), but is difficult to execute for AUVs, whose advantage lies in cruising.

With a flexible tail exostructure and a four-joint caudal fin driven by hydraulic power, vorticity control UUV (VCUUV) exhibits excellent maneuverability. It achieves a turning diameter of 2 BL (body length) and turning rate up to 75 deg/s (Anderson & Kerrebrock, 1997). Although the hull of SPC-III is completely rigid and only two joints drive the caudal fin, its tail structure enables the caudal fin to realize an offset angle from 0 to 90 deg. An offset angle of 90 deg can be used for emergency braking.

Figure 11 shows the circular trajectory of SPC-III and the comparison UUV in maneuverability experiments. The

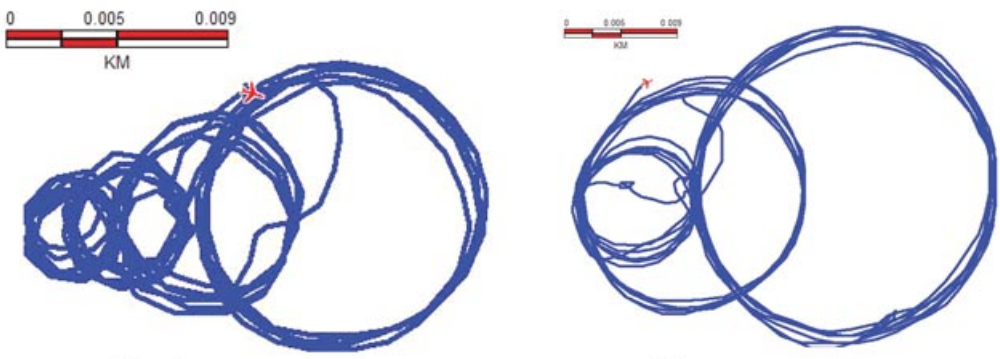

(a) SPC-III robotic fish (b) Comparison UUV

Figure 11. The trajectories of SPC-III robotic fish and the comparison UUV in maneuverability experiments.

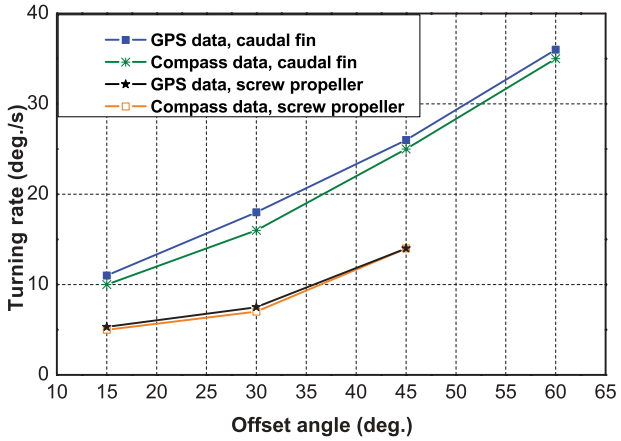

Figure 12. Turning rates of SPC-III and the comparison AUV, with translational speed of about 1.1 m/s.

trajectories are drawn using GPS data recorded by the autopilot. The flapping frequency of the caudal fin is 2 Hz, and the rotational speed of the screw propeller is 7.5 rps. The translational speeds of both vehicles are about 1.1 m/s. The caudal fin thruster achieves a minimum turning radius of 1 BL at a 60-deg offset angle, whereas the screw propeller, which uses a rudder, achieves a turning radius of 2.5 BL. Figure 12 shows the results of turning rate, including two sets of data. One set of data is obtained by counting the time the vehicle takes to finish the circular route, and the other is obtained according to compass data. At similar offset angles, the turning rate of the propeller-driven UUV is about one-half that of the fin-driven UUV.

5. PROBE EXPERIMENT ON BLUE-GREEN ALGAE

The propulsion and maneuverability performance of SPC-III in real-world application scenarios was examined in a mission to sample water quality and blue-green algae concentration. Located in the Changjiang Delta region, Taihu Lake is the major water source of Wuxi city. In the summer of 2007, there was a massive breakout of blue-green algae in Taihu Lake, which became a prime environmental issue

Table II. Data on water quality of Taihu Lake brought back by SPC-III carrying HACH D5X (November 2007).

Characteristic	Value
Average PH value	8.52
Maximum PH value	9.51
Concentration of blue-green algae (center of the lake)	3,823 cells/ml
Average pollution concentration (part of lake shore, red part in Figure 13)	288,112 cells/ml
Maximum concentration obtained (see Figure 14)	868,120 cells/ml

Figure 13. Cruising trajectories of SPC-III in the water quality probe experiment at Taihu Lake are shown in blue, and the areas under heavy pollution are indicated in red.

for both local residents and the government. In November 2007, carrying water quality multiprobes (HACH D5X), SPC-III successfully performed a probe cruise of about 49 km in Taihu Lake and brought back concentration data of blue-green algae. Some of the probe results are shown in Table II. Areas under heavy pollution are indicated by red in Figure 13. The place where the maximum concentration was obtained is shown is Figure 14.

As a portable AUV, the convenience of SPC-III was proven in the experiment in Taihu Lake. Figure 15 shows the working environment of SPC-III in Taihu Lake. It can be plunged or fished easily by two people manually without the use of special ships or devices. Aquatic plants near the bank are often a great threat to small propellers, but

Figure 14. The place where maximum concentration was obtained.

Figure 15. Working environment of SPC-III in Taihu Lake.

a caudal fin thruster that depends on oscillating propulsion can safely pass such areas. Thus SPC-III can cruise in water areas close to the bank and full of aquatic plants. Because blue-green algae are active in these areas, the maneuverability advantage of SPC-III is very remarkable. Furthermore, nets or navigation marks often appear on the set navigation route, which otherwise requires human intervention to change the course of the vehicle. Owing to its rapid turning rate, SPC-III can take action when it is very close to the obstacles and does not need early warning. As for the obtruding aquatic bushes it met when cruising in the area a few meters from the bank, SPC-III can avoid them with a very small turning radius by slowing down. This is very difficult for an AUV with a screw propeller.

Having its batteries charged only one time, SPC-III completed its 49-km mission intermittently in 3 days. On the first day, the robotic fish cruised 12 km. Both the stability of the propulsion system and the quality of water near the dock were tested. On the second day, the robotic fish cruised 16 km close to the city to obtain the water quality. On the third day, a journey of 21 km was performed gathering the water quality data near the bank of a tourism area. Heavy pollution of blue-green algae was found in the above areas. No fault was observed on the caudal fin thruster. The reliability of this kind of propeller was preliminarily confirmed.

6. DISCUSSION

Compared with dolphin and tuna, which swim at high speed, the current biorobotic UUV still has a long way to go. Yet compared with a conventional screw-propelled AUV, SPC-III has made great progress. With small displacement tonnage, the caudal fin can generate vector thrust and increase the low-speed maneuverability of an AUV remarkably. In addition, the power of the caudal fin thruster is satisfying. The two-joint caudal fin thruster driven by dc servomotors has been proven to be a feasible solution to biomimetic underwater propulsion. Of course, there also exist some inherent deficiencies. For example, the actuating motors work in an oscillation condition, which determines that the peak power is 40% higher than that in uniform rotation in order to achieve similar power output. As a result, the actuating motor and amplifier have to possess higher power redundancy, thus reducing the power density of the propeller. This is the exact reason why the vehicle velocity of SPC-III is hard to increase. Working in an oscillation condition also prevents the actuating motors and reducer from working continuously at optimum efficiency points. It is foreseeable that both electromechanical conversion efficiency and transmission efficiency of the caudal fin thruster are lower than that of a screw propeller, which works in uniform rotation.

7. CONCLUSIONS AND FUTURE WORK

This paper presented an alternative design scheme with a two-joint caudal fin thruster for a portable AUV to a single-screw propeller. With this kind of caudal fin thruster, the displacement of a SPC-III robotic fish is 47 kg and its length is 1.75 m. The caudal fin thruster accounts for only 7% of the vehicle displacement. Owing to the improvement on the mechanical structure and motion control algorithm of the tail fin, SPC-III shows much better performance than SPC-II. An experimental comparison of propeller-based and flapping-fin propulsion efficiency was carried out at sea. At the speed of 1.1 m/s, the caudal fin thruster consumed about 7% less power than the screw propeller. The maximum speed for the caudal fin design reached 1.36 m/s, and the minimum turning radius was 1 BL. When powered by 14 168-Wh batteries, the endurance was about 20 h at a speed of 2 kn. SPC-III successfully performed a 3-day mission, cruising about 49 km in Taihu Lake, which validated the reliability and high maneuverability of the caudal fin thruster, indicating that SPC-III can work in highly polluted and complicated environments.

In this study, experimental results of long-term operations with the caudal fin propulsion in a real-world lake environment were reported for the first time. With the same tonnage, hydrodynamic shape, and speed, the performances of the caudal fin thruster and a conventional screw propeller were compared. The empirical finding was that the biomimetic propulsion can achieve performances similar to that of a screw propeller in terms of efficiency and the fraction of displacement but greater maneuverability can be realized with the caudal fin thruster. These results will play a guiding role in the development of next-generation UUVs that merges biomimetic and conventional designs.

Future research will be carried out in the following three areas. First, power consumption and efficiency of the caudal fin at higher speed will be investigated, which

requires servo drive systems with higher power densities to be developed. Second, an adaptive control algorithm of the caudal fin that adjusts flapping movements according to the dynamics of the surrounding fluid will be explored. Third, movements in three-dimensional space will be realized with multiple pectoral fins that generate vector thrust. These promising research directions will produce some useful and exciting results in the near future.

APPENDIX: INDEX TO MULTIMEDIA EXTENSIONS

The videos are available as Supporting Information in the online version of this article.

Extension	Media type	Description
1	Video	The screw-driven UUV swimming at 1.1 m/s with rotational speed of 5 rps
2	Video	SPC-III robotic fish swimming at 1.0 m/s with flapping frequency of 2 Hz
3	Video	SPC-III performing fast turning with small radius

ACKNOWLEDGMENTS

The research work on the screw propeller was conducted with the help of the China Ship Scientific Research Center (CSSRC). The authors would like to thank the referees for careful reading of the manuscript and for their valuable comments.

REFERENCES

Anderson, J. M., & Kerrebrock, P. A. (1997, September). The vorticity control unmanned undersea vehicle (VCUUV)—An autonomous vehicle employing fish swimming propulsion and maneuvering. In Proceedings of 11th International Symposium on Unmanned, Undeterred Submersible Technology, Durham, NH (pp. 189–195).

Anderson, J. M., Streitlien, K., Barrett, D. S., & Triantafyllou, M. S. (1998). Oscillating foils of high propulsive efficiency. Journal of Fluid Mechanics, 360, 41–72.

Barrett, D. S., & Triantafyllou, M. S. (1999). Drag reduction in fish-like locomotion. Journal of Fluid Mechanics, 392, 183–212.

Chen, D., Wang, T., Liang, J., & Wang, T. (2008, February). The design and application of a sUAV system for Antarctic expedition. In Proceeding of the 2008 International Conference on Robotics and Biomimetics, Bangkok, Thailand (pp. 1129–1134).

Hu, H., Liu, J., Duks, I., & Francis, G. (2006, October). Design of 3D swim patterns for autonomous robotic fish. In Proceedings of the 2006 IEEE/RSJ International Conference on Intelligent Robots and Systems, Beijing (pp. 2406–2411).

iRobot Maritime Robots—Transphibian (2010). Retrieved May 20, 2010, from http://www.irobot.com/gi/maritime/Transphibian/.

Liang, J., Wang, T., Wang, S., Zou, D., & Sun, J. (2005, August). Experiment of robofish aided underwater archaeology. In Proceeding of the 2005 International Conference on Robotics and Biomimetics, Hong Kong (pp. 231–235).

Mbemmo, E., Chen, Z., Shatara , S., & Tan, X. (2008, May). Modeling of biomimetic robotic fish propelled by an ionic polymer–metal composite actuator. In Proceedings of the 2008 IEEE International Conference on Robotics and Automation, Orlando, FL (pp. 689–693).

Wang, T., & Liang, J. (2005, August). Stabilization based design and experimental research of a fish robot. In Proceedings of the 2005 IEEE/RSJ International Conference on Intelligent Robots and Systems, Edmonton, Canada (pp. 954–959).

Ying, L., & Zhu, J. (2006). Screw design and implementation on comparison UUV (Tech. Rep. 20070145). China Ship Scientific Research Center.